J. Indian Inst. Sci. 66, Aug. 1986, pp. 555–571
© Indian Institute of Science, Printed in India.

IISc THESES ABSTRACTS

Thesis Abstract (Ph.D.)

Structure and properties of lead oxyhalide glasses by B. Govinda Rao.
Research supervisor: K. J. Rao
Department: Solid State and Structural Chemistry Unit.

1. Introduction

Covalent and ionic glasses have several differences in their structures and properties. For instances, local structures in covalent glasses are characterized by low coordination while ionic glasses are characterized by high coordinations. With increasing ionicity the bonding becomes nondirectional which leads to higher coordinations. Glasses based on PbO-PbF_2 and PbO-$PbCl_2$ systems are very interesting since nature of bonding may be changed in the same system. PbO is covalently bonded while $PbCl_2$ of PbF_2 are ionic. Therefore, different compositions of these glasses are expected to possess different degrees of ionicity of bonding. Hence the effect of nature of bonding on the structure and properties of glasses can be studied by investigating lead oxyhalide glasses.

2. Experimental

PbO-PbF_2 and PbO-$PbCl_2$ glasses have been prepared by melting appropriate quantities of AnalaR grade Pb_3O_4 and PbF_2 or $PbCl_2$. Densities and microhardnesses and thermal properties such as heat capacity, C_p, glass transition temperature, T_g, crystallization temperature, T_{cr}, and change in heat capacity, ΔC_p at T_g have been measured. The methods for these measurements are described elsewhere[1,2]. X-ray diffraction intensity data were collected on a Philips X-ray diffractometer. The corrected intensity data were Fourier transformed to obtain pair distribution functions (PDFs). EXAFS above the L_3-edge and XANES associated with all the L-edges were recorded at CHESS synchroton facility and analysed as reported elsewhere[3,4]. For ESR and optical studies, these glasses were doped with 0.5 mol%, Fe_2O_3 and MnO. ESR spectra were recorded on a Varian E-109 spectrometer. Optical spectra were recorded on a Pye Unicam (SP1-800) UV-visible spectrometer. Emission and excitation spectra were recorded on a Shimatzu (RF 510) spectrometer. Effect of temperature and pressure on the electrical resistivity of these glasses were measured by the methods reported elsewhere[1,5].

3. Results and discussion

PbO-PbF_2 and PbO-$PbCl_2$ systems form glasses in the ranges of 80 to 30 mol% PbO and 90 to 50 mol% PbO respectively[1,2]. Glass formation range is more extensive in PbO-PbF_2 system than in PbO-$PbCl_2$ system, particularly on the PbX_2-rich site. It is probably due to the ability of fluoride ions to participate in network formation. The densities vary linearly with composition in both the

systems. The behaviours of C_p and ΔC_p seem to suggest that ionicity of bonding varies with composition in these glasses. Values of microhardnesses of glasses in both the systems decrease with increasing PbX_2 content indicating that ionicity of bonding increases with increasing PbX_2 content. Variation of T_g for both the systems is consistent with the cluster model of glasses. Temperature variation of d.c. conductivity of these glasses show that F^- ions are the conducting species in the case of PbO-PbF_2 glasses.

The structure of PbO-PbX_2 glass have been investigated by X-ray diffraction[1-6]. The PDFs for PbO-PbF_2 glasses are almost similar for all compositions. The PDFs for PbO-$PbCl_2$ glasses are also similar except for the variations in the position and intensity of the first peak with composition. The position and intensity of the second peak around 4.0 Å which is mainly due to Pb-Pb pair correlation remains unaffected by composition in both the systems. This feature of PDFs suggests the presence of a common motif of packing in all glass compositions. These insights along with the knowledge of crystal structures of related compounds such as Pb_2OF_2 and $Pb_3O_2Cl_2$ (mendipite) have been used to develop a structural model of PbO-PbX_2 glasses.

The main features of the structural model are as follows: (1) Covalent -O-Pb-O- linkages are present in all glass compositions and are considered essential for glass formation. (2) Oxygen atoms are present in $[OPb_4]$ type of (distorted) tetrahedra and are primarily responsible for establishing network features through covalent bonding. (3) Lead atoms possess an anionic coordination of six (a coordination very similar to that of lead in Pb_2OF_2 and $Pb_3O_2Cl_2$ compounds) in all glasses. Therefore, it has been suggested that $[PbO_2X_4]$ type of octahedra are present in the entire glass forming ranges of the two systems. These octahedra may be quite distorted. (4) The coordination number of halogens varies with composition, being high in PbO-rich glasses and low in PbX_2-rich compositions as it is required by conditions of electrical neutrality (or bonding rules).

The structural model is consistent with all the features of the PDFs. A preliminary neutron diffraction study[7] of PbO-$PbCl_2$ glasses also supports the structural model.

The EXAFS associated with the Pb-L_3 edges of these glasses have been analysed to establish the local coordination of Pb in these glasses[3]. Structural parameters (bond distances and coordination numbers) of the first coordination shell of Pb in PbO-PbX_2 glasses obtained from this analysis indicate that the coordination number of lead is close to six in all glass compositions and that the coordination is made up of approximately two oxygens and four chlorines. This establishes the structure postulated on the basis of X-ray diffraction studies.

The nature of bonding in PbO-PbF_2 glasses has been investigated by XANES analysis of the L-edge of Pb[4]. Since the ionicity of bonding seems to increase with increasing-PbF_2 content, it should be expected that the symmetry of $[PbO_2F_4]$ units also increases with PbF_2 content. By invoking symmetry-based Molecular Orbital (MO) theory, variation of XANES features of all the L-edges of Pb in these glasses have been shown to be consistent with increase of symmetry of $[PbO_2F_4]$ units from C_s through C_{2v} to D_{4h} with increasing PbF_2 content. The white line intensities, of the edges exhibit a decreasing trend with increasing PbF_2 content, suggesting an increase in ionicity of bonding. The calculations of intensities yield an estimate of about 22–32% change in ionicity in the composition change of 20–60 mole% PbF_2.

The ESR spectra of doped Fe^{3+} and Mn^{2+} ions in PbO-PbX_2 glasses[8] show that these ions are present mostly in isolated low (rhombic) symmetry sites in these glasses. In the case of Fe^{3+} ions, ESR spectra of PbO-PbF_2 glasses are not affected by composition while the spectra of PbO-$PbCl_2$ glasses are affected quite drastically. The spectra of Mn^{2+} are affected by composition in both the systems; more drastically in PbO-$PbCl_2$ glasses than in PbO-PbF_2 glasses. Further, ESR spectra of Mn^{2+} ions in PbO-PbF_2 glasses are similar to those in oxide

glasses whereas the Mn^{2+} spectra in PbO-$PbCl_2$ glasses are similar to those in chalcogenide glasses. These differences in the spectra of the two transition metal ions in the two glass systems seem to result from at least three important causes: (1) Due to its high ionic potential Fe^{3+} ion acquires its own environment in contrast to Mn^{2+} ion which substitutes for Pb^{2+} ion in these glasses. (2) Because of the similarities in sizes and nephelauxetic effects of O^{2-} and F^- ions, Mn^{2+} ions acquire more symmetrical environment in fluoride glasses than in chloride glasses. (3) Increase in halide ion concentration increases the ionicity of bonding and favours more symmetrical environment around dopant ions, which causes the observed compositional dependence of the spectra.

ESR studies of the glasses containing higher concentrations of dopant ions indicate that a fraction of these ions are still present as isolated ions and also a considerable fraction of manganese is in Mn^{3+} state in these glasses. These aspects have been investigated by optical spectroscopy[9] and magnetic susceptibility[10]. Optical studies show that both Mn^{2+} and Mn^{3+} ions are present in octahedral sites. Magnetic susceptibility behaviour suggests that interaction between transition metal ions in lead oxyhalide glasses are predominantly antiferromagnetic.

Glasses of both the systems have been found to undergo crystallization under pressure as indicated by the sudden drop in the normalized resistivities in all the cases[5]. Pressure-induced transitions in PbO-PbF_2 glasses exhibit a first order like behaviour while those in PbO-$PbCl_2$ glasses possess features of a continuous transition. Further, the activation volumes of the two systems computed from the initial linear rise of normalized resistivity as a function of pressure exhibit opposite trends. These differences have been attributed to the differences in the ionic sizes and mobilities of F^- and Cl^- ions and also to pressure-induced modification of Pb-O bonding.

The glasses in PbO-PbX_2 systems are therefore quite novel in view of the continuous variation in the nature of bonding and also in view of the presence of an octahedral motif in the structure of all glass compositions.

References

1. GOVINDA RAO, B., SUNDAR, H. G. K. AND RAO, K. J. — *J. Chem. Soc. Faraday Trans.* I, 1984, **80**, 3491.
2. RAO, K. J., RAO, B. G. AND ELLIOTT, S. R. — *J. Mater. Sci.*, 1985, **20**, 1678.
3. RAO, K. J., WONG, J. AND RAO, B. G. — *Phys. Chem. Glasses*, 1984, **25**, 57.
4. RAO, K. J., RAO, B. G. AND WONG, J. — *J. Chem. Phys.*, (communicated).
5. RAO, K. J., PARTHASARATHY, G., RAO, B. G. AND GOPAL, E. S. R. — *Mater. Res. Bull.*, 1984, **19**, 1221.

6. Rao, B. G. and Rao, K. J.	*Phys. Chem. Glasses*, 1984, **25**, 11.
7. Wright, A. C., Grimley, D. I., Sinclair, R. N., Rao, K. J. and Rao, B. G.	*J. Physique*, 1985, **C8**, 307.
8. Rao, B. G. and Rao, K. J.	*Chem. Phys.*, 1986, **102**, 121.
9. Rao, B. G. and Rao, K. J.	*J. Mater. Sci. Lett.*, 1986, **5**, 141.
10. Rao, B. G., Vasanthacharya, N. Y. and Rao, K. J.	*Proc. Indian Acad. Sci. (Chem. Sci.)*, 1986, **96**, 383.

Thesis Abstract (Ph.D.)

Transformation of progesterone by fungal systems: Studies on the 11α-hydroxylase system from *Aspergillus ochraceus* by Jayanti Srivatsan.
Research supervisor: K. M. Madyastha.
Department: Organic Chemistry.

1. Introduction

Microbial hydroxylations of steroids have gained industrial importance since these reactions a commonly used in the synthesis of pharmaceutically important steroid hormones which a sometimes difficult to synthesize by the conventional chemical routes. Various fungi of t genera, *Aspergillus* and *Rhizopus* have been shown to hydroxylate progesterone and relat steroids at 11α-position[1-3]. There are innumerable reports on this transformation. Howev there are very few reports pertaining to the nature of the enzyme system involved in this speci hydroxylation[2,4-7]. In the present study, the enzyme system of *Aspergillus ochraceus* involved the conversion of progesterone to 11α-hydroxyprogesterone has been studied in great deta

2. Results and discussion

The optimal conditions for higher 11α-hydroxylase activity with conidia and vegetative cells of *A ochraceus* were established. Among the different steroids tested for their ability to induce th hydroxylase system, progesterone was found to be the best inducer. The inducible nature of th hydroxylase activity was further supported by its inhibition by cycloheximide added during th induction period.

The ideal conditions to obtain maximum hydroxylase activity in the cell-free extract wer ascertained. Tris-HCl (0.1 M, pH 8.3) buffer containing glycerol (10%, w/v), EDTA (10 mM) an DTT (5 mM) was required to obtain very active cell-free extract. The 11α-hydroxylase activity wa found to be solely localised in the microsomal fraction. This constitutes the first report on th

intracellular localisation of this hydroxylase system from the fungi. Although the pH required to obtain active cell-free extract was 8.3, the hydroxylase had a pH optimum of 7.7. The hydroxylation reaction required NADPH as the cofactor and molecular oxygen. The microsomes obtained from the induced mycelium of *A. ochraceus*, under the optimal conditions, converted 85–90% of the added progesterone to 11α-hydroxyprogesterone in the presence of NADPH and O_2. The uninduced microsomes did not show any hydroxylase activity. The hydroxylase activity was inhibited by metyrapone, CO and SKF-525 A, the inhibitors of cytochrome P-450, indicating the possible involvement of cytochrome P-450 in the hydroxylation reaction. The inhibition of the hydroxylase by cytochrome *c* and the presence of high levels of NADPH-cytochrome *c* reductase in the induced microsomes showed its possible involvement in the hydroxylation reaction. Phospholipases (C and D) did not inhibit the microsomal hydroxylase activity. The cytochrome P-450 in the microsomes when treated with the substrate, progesterone, elicited a Type I spectrum (λ max 386 nm; λ min 415 nm). Substrate specificity studies indicated that the hydroxylase system accepts only Δ^4-3-keto steroids as substrates.

A simple method was developed for the isolation of microsomes from the post-mitochondrial supernate of the induced mycelium of *A. ochraceus* by aggregation with Ca^{2+} ions. The various enzyme activities of the microsomes obtained by Ca^{2+} aggregation clearly indicated this method to be an alternative for ultracentrifugation method. This method has been used for the first time to isolate microsomes from a fungus.

The membrane bound hydroxylase was solubilised using various ionic and non-ionic detergents. The non-ionic detergent, Tween-80, was found to be the most efficient detergent and Tween-80 solubilized membrane fraction contained high levels of cytochrome P-450, NADPH-cytochrome *c* reductase and hydroxylase activities. Various biochemical techniques were tried to resolve cytochrome P-450 and NADPH-cytochrome *c* reductase. These proteins were separated and partially purified by ω-aminohexyl sepharose 4 B column chromatography. Attempts to reconstitute the hydroxylase system with the partially purified proteins (in the absence or presence of phospholipid) were not successful. Even the partialiy purified cytochrome P-450 failed to carry out the hydroxylation in the presence of $NaIO_4$, H_2O_2 and other peroxides. The experiments could not conclusively show whether a two-or a three-protein component system is involved in the hydroxylation reaction. Various kinetic parameters of the partially purified NADPH-cytochrome *c* reductase were determined. These studies indicated that the reductase is different from other purified reductases isolated from different sources. The reconstitution of the 11α-hydroxylase system would unequivocally establish the components involved in the 11α-hydroxylation reaction.

2.1 *Transformation of progesterone by a Mucor sp.*

The fungi of the genera, *Mucor* have been shown to hydroxylate steroids and cardenolides at various positions. Many of the reports regarding the transformations by Mucorales are patented. The mode of transformation of progesterone by a *Mucor* sp. isolated from the soil was studied. At least eight metabolites were formed of which four were in major amounts. Five metabolites were isolated, purified and identified by various spectral analyses (uv, ir nmr & mass). The major metabolites were 14α-hydroxyprogesterone, 7β, 14α-dihydroxyprogesterone, 7α, 14α-dihydroxyprogesterone and 6β, 14α-dihydroxyprogesterone, while 5β, 14α-dihydroxypregnane-3,20-dione was the minor metabolite formed. The hydroxylation of steroids at 5β- or 7β-position has not been reported so far by any *Mucor* species. The time course experiments carried out with the radiolabelled progesterone suggested 14α-hydroxyprogesterone as the first metabolite formed during the transformation which was further converted into the dihydroxy metabolites. This

assumption was further supported by direct evidence; the *in vitro* conversion of progesterone to 14α hydroxyprogesterone in the presence of NADPH. The studies on the enzymes involved in the transformation would establish the sequence of the hydroxylation reaction.

References

1. Peterson, D. H. and Murray, H. C. — *J. Am. Chem. Soc.*, 1952, 74, 1871–1872
2. Shrivastava, M., Moody, J. A. and Smith, L. L. — *Biochim. Biophys. Acta*, 1970, 202, 172–179
3. Bhargavat, K. and Hudnik-Plevnik, T. — *Biochem. Biophys. Res. Commun.*, 1977, 74, 1192–1198.
4. Bhargavat, K. and Hudnik-Plevnik, T. — *J. Steroid Biochem.*, 1981, 14, 395–399
5. Ghosh, D. and Samanta, T. B. — *J. Steroid Biochem.*, 1981, 14, 1063–1067
6. Jayanthi, C. R., Madyastha, P. and Madyastha, K. M. — *Biochem. Biophys. Res. Commun.*, 1982, 106, 1262–1268.
7. Madyastha, K. M., Jayanthi, C. R., Madyastha, P. and Sumathi, D. — *Can. J. Biochem. Cell Biol.*, 1984, 62, 100–107

Thesis Abstract (Ph.D.)

Kinetics and mechanism of anodic oxidation of chlorate ion to perchlorate ion on lead dioxide electrode by N. Munichandraiah.
Research supervisor: S. Sathyanarayana.
Department: Inorganic and Physical Chemistry.

1. Introduction

Electrolytic preparation of inorganic and organic compounds is of growing importance due to its ecological compatibility as well as its requirement of minimum energy under proper conditions of operation. For such electrosynthetic applications, one of the important components is the anode material[1]. The base metal oxides such as Co_3O_4, PbO_2, MnO_2, etc., coated on a suitable substrate such as Ti are of particular technological importance as insoluble anodes due to their inherently low cost. The use of a conducting support leads, primarily, to a new problem viz., that of adhesion between the support and the coating, without causing any significant ohmic drop. The second problem which arises with the use of the base metal oxide anodes is that of enhancing the surface area of the oxide.

In the present work, a new process has been developed to overcome the above problems, and applied to the preparation of insoluble anodes of β-lead oxide with a fine pore structure on the

outer surface (*i.e.*, solution side), low porosity on the inner surface (*i.e.*, substrate side), strong adhesion to titanium substrate, and good cohesion within the coating. These results have been achieved in the present work by the addition to the PbO_2 coating solution, of a foaming agent, Teepol (a mixture of sodium sec. alkyl sulphates, $C_nH_{2n+1}CH(CH_3)OSO_3Na$ where n = 6 to 16).

The anodic oxidation of chlorate ion to perchlorate ion *viz.*,

$$ClO_3^- + H_2O \rightarrow ClO_4^- + 2H^+ + 2e^- \qquad (1)$$

is of considerable importance technologically as well as from a scientific point of view. A study of the available literature on kinetics and mechanism of reaction[1] reveals that the mechanisms suggested are either simply speculated upon, or based on indirect data which do not exclude other possible mechanisms. In the present studies, systematic kinetic investigations have been carried out in order to elucidate the mechanism of this reaction.

2. Experimental programme

In order to characterise the porous β-PbO_2(Ti) electrodes, physical studies such as porosity, X-ray powder diffraction, SEM and BET area and electrochemical studies such as open-circuit potential measurements, galvanostatic anodic-charging curves and galvanostatic-anodic Tafel polarisation measurements in 0.2 M solution of sodium sulphate have been carried out.

In the present investigation kinetic analyses including double layer effects for several possible mechanisms of reaction (1) have been carried out, diagnostic criteria have been deduced. The final form of the rate equation derived for a rate determining step in any of the postulated mechanisms is as follows:

$$\ln(-i) = \text{constant} + p \ln c^0_{ClO_3^-} - r \ln J + s\,\text{pH} + t\,E$$

where,

$$p = \frac{\partial \ln(-i)}{\partial \ln c^0_{ClO_3^-}}\ ;\ r = \frac{\partial \ln(-i)}{\partial \ln J}\ ;\ s = \frac{\partial \ln(-i)}{\partial \text{pH}} \text{ and } t = \frac{\partial \ln(-i)}{\partial E}.$$

The values of p, r, s and t have been obtained experimentally from steady-state galvanostatic polarisation measurements, after correcting the current for the oxygen evolution reaction at each anode potential.

3. Main results and conclusions

The data obtained from anodic-charging curves and Tafel plots have been used to evaluate the surface area of porous β-PbO_2(Ti) electrodes relative to the surface area of compact β-PbO_2(Ti) and platinised titanium electrodes. For this purpose, the charging curves have been analysed for double-layer capacitance, after correcting the charging current for any faradaic current that may be present. The double-layer capacitance C_d, at a chosen potential E* is then obtained as

$$C_{d,E^*} = \frac{i_2 - i_1}{\left(\frac{dE}{dt}\right)_{1,E^*} - \left(\frac{dE}{dt}\right)_{2,E^*}}$$

where $\left(\frac{dE}{dt}\right)_{i_1}$ and $\left(\frac{dE}{dt}\right)_{i_2}$ are the derivatives of the galvanostatic-charging curves at the current densities i_1 and i_2 respectively. The capacitances of porous β-PbO_2(Ti) electrodes are several times higher in comparison with Pt(Ti) electrodes, which may be attributed to a proportionate increase in the effective area of the porous PbO_2 electrodes. The area enhancement factor, as calculated from the capacitance data near the open-circuit potentials, is about 40 for porous β-PbO_2(Ti) electrode of 1.0 mm thick coating, about 15 for porous β-PbO_2(Ti) electrode of 0.5 mm thick coating and about 2 for compact β-PbO_2(Ti) electrodes of both 1.0 mm and 0.5 mm thick coating, assuming that the capacitance value for the smooth platinised titanium electrode corresponds to a surface of zero roughness. From anodic polarisation data in Na_2SO_4 solution, well-defined Tafel plots of about 150 mV slope extending over two decades of current are obtained in all the cases. The values of the exchange current densities derived are about 0.03 A/cm^2 for porous β-PbO_2(Ti) electrode (0.5 mm or 1 mm thick) and about 0.002 A/cm^2 for compact β-PbO_2(Ti) electrode (0.5 mm or 1 mm thick). In other words, the porous β-PbO_2(Ti) electrode is about fifteen times more active electrochemically than the compact β-PbO_2(Ti) electrode for oxygen evolution reaction under the same conditions. Considering that the area-ratio of the two electrodes as deduced from the double-layer-capacitance data is of the same order of magnitude as the ratio of exchange current densities on these electrodes, the enhanced electrocatalytic activity of porous β-PbO_2(Ti) anodes may be expected to prevail also for other reactions such as chlorate or perchlorate electrosynthesis.

From the polarisation data obtained for chlorate oxidation alone, well defined Tafel lines are obtained with a slope of 0.30 ± 0.02 V, after applying due correction for the ohmic drop. This Tafel slope leads to the value of $t \approx 7.7 \pm 0.5\ V^{-1}$. The values of p, r and s are also obtained from the corrected polarisation curves as 0.12, 1.25 and 0.0 respectively. On comparing these values of kinetic parameters with the values predicted for each postulated mechanism, it is found that only two out of eighteen mechanisms proposed show an acceptable fit with the experimental data. They are:

(1) $H_2O \rightarrow (OH)_{ad} + H^+ + e^-$

$ClO_3^- + (OH)_{ad} \rightleftharpoons ClO_4^- + H^+ + e^-$

(2) $ClO_3^- \rightleftharpoons (ClO_3)_{ad} + e^-$

$H_2O \rightarrow (OH)_{ad} + H^+ + e^-$

$(ClO_3)_{ad} + (OH)_{ad} \rightleftharpoons ClO_4^- + H^+$

Both these mechanisms involve oxidation of water in a one-electron transfer step to give adsorbed (OH) radical as the rate-determining step.

1. KUHN, A. T. *Industrial electrochemical processes*, Elsevier Publishing Company, New York, 1971

Thesis Abstract (Ph.D.)

Synthesis and conformational analysis of cyclic cystine peptides by Raghuvansh Kishore.
Research supervisor: P. Balaram.
Department: Molecular Biophysics Unit.

1. Introduction

Disulfide bridges formed between two cysteine residues (Cys) which are far apart in the primary structure, may result in the stabilization of loops in the polypeptide chain. Small disulfide loops of the type -Cys-(NH-CH-CO)$_n$-Cys-, where $n = 0, 1, 2, 3$ or 4, are frequently observed in many

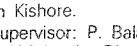

proteins, polypeptide hormones and toxins. Small disulfide loops have also been shown to constitute the active sites of various redox proteins, which function *via* reversible disulfide-dithiol redox processes. Despite their widespread occurrence and undoubted importance there have been relatively few investigations on the conformational properties of cyclic peptide disulfides[1].

In the present investigation, 11, 17 and 20-membered cyclic cystine peptides and 22-membered cyclic biscystine peptides have been synthesized and subjected to detailed spectroscopic analysis. 14-Membered cyclic peptide disulfides, which correspond to the active sites of the redox-proteins thioredoxins and glutaredoxins[2,3] have also been investigated. The major goal of this thesis has been to delineate the conformational characteristics of cyclic peptide disulfides having limited ring sizes (11- to 22-membered rings).

2. Experimental methods

Peptides were synthesized by standard solution phase procedures using dicyclohexylcarbodiimide (DCC) or 1-hydroxybenzotriazole (HOBt)/DCC-mediated coupling. The *t*-butyloxycarbonyl (Boc), methylamide ($NHCH_3$) and benzyl (Bzl) groups were used for amino, carboxyl and thiol protection, respectively. The disulfides were prepared, first by debenzylation using Na/liquid ammonia procedure followed by cyclic oxidation using $K_3Fe(CN)_6$ solution, in aqueous medium at pH 6.8–7.0[4]. Characterization of peptides at every stage of synthesis was performed by 60 MHz, 80 MHz and 270 MHz ^{1}H NMR. All final peptide disulfides were purified by silica gel column chromatography using $CHCl_3$ or CH_3OH–$CHCl_3$ mixtures and shown to be homogeneous by high performance liquid chromatography (HPLC) on a reverse phase C-18 column. The monomeric or dimeric structures of the peptide disulfides were established by observation of the molecular ion peak in fast atom bombardment (FAB) mass spectra.

Conformational studies of the peptide disulfides were carried out by using ^{1}H NMR, CD, IR and fluorescence spectroscopic methods. In several cases, structures have been confirmed by Nuclear Overhauser Effect (NOE) measurements.

3. Results and conclusions

Oxidative cyclization of the tripeptide dithiol Boc-Cys (SH)-X-Cys (SH)-$NHCH_3$ yielded products of both dimeric and monomeric structures. The dimeric products

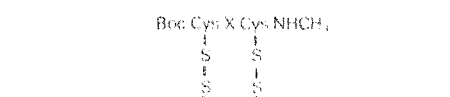

X = L-Ala
X = D-Ala

(cyclic biscystine peptides) serve as excellent models for antiparallel β-sheet conformations[5]. Distinctive NMR spectral parameters like lowfield C$^{\alpha}$H resonances and high coupling constants (^{3}HNC$^{\alpha}$H) are characteristic features of these peptides. A novel CD spectral pattern (strong positive band at ~ 226 nm) has been observed in various solvents. On the other hand, the monomeric cyclic cystine peptide Boc-Cys-L-Ala-Cys-NHCH$_3$ adopts a γ-turn conformation

stabilized by two (1 ⇢ 3 and 3 ⇢ 1) intramolecular hydrogen bonds[6].

The studies on two 17-membered cyclic peptide disulfides Boc-Cys-X-Y-Gly-Cys-NHCH$_3$ where

X-Y = Gly-Leu or Ala-Aib provide evidence for a γ-turn at the central residue followed by a β-sheet-like extended structure.

Detailed conformational analysis of the 20 membered cyclic peptide disulfide, Boc-Cys-Val-Aib-

Ala-Leu-Cys-NHCH$_3$ establishes that the molecule adopts an intramolecular antiparallel β-sheet

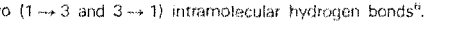

conformation, generated by means of a chain reversal involving an Aib-Ala Type I′ β-turn. The presence of three intramolecular hydrogen bonds and an extended conformation at the Val, Leu and Cys residues was established by NMR spectroscopy using solvent dependence of NH chemical shifts and by the observations of successive C$^{\alpha}$H ↔ NH interresidue NOEs.

Studies on 14-membered cyclic peptide disulfides, corresponding to the active sites of *redox-proteins thioredoxins and glutaredoxins have shown that the model* peptide disulfide Boc-Trp-Cys-Gly-Pro-Cys-NHCH$_3$ (*E. coli* thioredoxin active site) adopts a consecutive β-turn

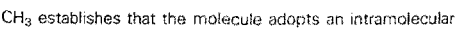

conformation involving the Cys(5) and methylamide NH groups. On the other hand, the peptide Boc-Cys-Val-Tyr-Cys-NHCH$_3$ (phage T4 thioredoxin active site) favours a non β-turn conformation.

Particularly, interesting results were obtained while studying the conformation of Boc-Cys-Pro-Tyr-Cys-NHCH$_3$ (glutaredoxin active site) and its analog Boc-Cys-Pro-Phe-Cys-NHCH$_3$. In

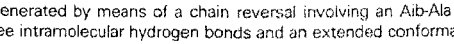

$CDCl_3$, these peptides adopt a Type I β-turn conformation, involving the Cys(4) NH in an intramolecular hydrogen bond. However, in $(CD_3)_2SO$ each peptide exhibits two distinct species

in slow exchange on the NMR time scale. The role of the aromatic residue at the third position as a structural determinant has been emphasized in these sequences.

The effect of addition of a disulfide reducing agent, dithiothreitol (DTT), on the fluorescence emission spectra of these peptides has clearly indicated that the aromatic fluorophores Trp/Tyr are significantly quenched by the proximate disulfide bridge[7]. Thus, these peptides serve to mimic the spectral changes that occur on reduction on the active site disulfide bridge in the native proteins, thioredoxin and glutaredoxin.

The results described in this thesis emphasize the utility of disulfide bridges in stabilizing specific peptide backbone conformations in cyclic peptide disulfides having limited ring size. Figure 1 summarizes the various well defined intramolecularly hydrogen-bonded conformations established in small cyclic cystine peptides.

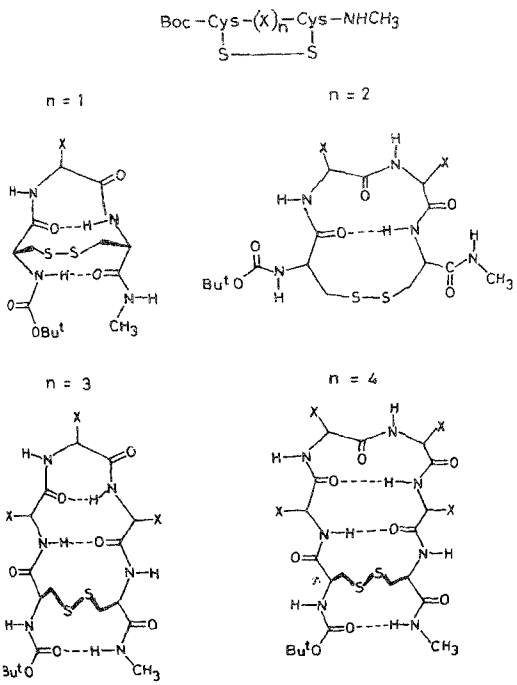

Fig. 1. Folded, hydrogen-bonded structures suggested for small disulfied loops (11- to 20-membered).

References

1. BALARAM, P. *Proc. Indian Acad. Sci (Chem. Sci.)*, 1984, **93**, 703.
2. HOLMGREN, A. *Curr. Topics Cellular Regulation*, 1981, **19**, 47.
3. HOLMGREN, A. *Ann. Rev. Biochem.*, 1985, **54**, 237.
4. SCHON, I. *Chem. Rev*, 1984, **84**, 287.
5. KISHORE, R., KUMAR, A. AND BALARAM, P. *J. Am. Chem. Soc.*, 1985, **107**, 8019.
6. KISHORE, R. AND BALARAM, P. *Biopolymers*, 1985, **24**, 2041.
7. KISHORE, R. AND BALARAM, P. *Thioredoxin and glutaredoxin systems: Structure and function*, Proc. 9th Nobel Conf., Raven Press, New York (in press).

Thesis Abstract (Ph.D.)

Facile routes to substituted di- and triformylbenzenes (Part I). Synthesis of pterosin-M and onitin (Part II) by B. Raju.
Research supervisor: G. S. Krishna Rao.
Department: Organic Chemistry.

A large variety of simple olefins and conjugated dienes are known to undergo Vilsmeier reaction[1]. The subdued reactivity of alkyl-substituted benzenes towards Vilsmeier reagent is well known and when the reaction occurs monosubstitution of the electrophilic Vilsmeier complex is a general rule. The availability of a large variety of alkylcyclohexadienes, by Birch reduction[2] of the corresponding aromatics, led us to examine their reactivity towards the Vilsmeier reagent. The investigation provided an attractive method for the synthesis of a variety of alkyl, alkoxy and chloro-substituted polyformylbenzenes which are not easily obtainable otherwise.

Open-chain enol ethers with a free β-position are easily accessible to attack by Vilsmeier complex[1]. Cyclic dienol ethers like the various 1-methoxy-1,4-cyclohexadienes, prepared from substituted anisoles by Birch reduction[2], were treated with the Vilsmeier reagent to give polyformylchlorobenzenes and this investigation resulted in a facile and direct method for the preparation of several polyformylchlorobenzenes[3].

Arnold's findings[1] of Vilsmeier reaction on carboxylic acids enlarge further the scope of the reaction. Under Vilsmeier reaction conditions substituted 1-carboxy-2,5-cyclohexadienes, obtained by Birch reduction[2] of corresponding aromatics, afforded various di- and triformylbenzenes[4]. The results are of interest not only from the mechanistic point of view, but also from their preparative value.

Known instances of *in situ* formation of cyclic products under Vilsmeier[1] reaction conditions in the literature have been less common. Vilsmeier formylation of carboxylic acids of type RCH_2CO_2H gave malonaldehydes with simultaneous decarboxylation. Substituted polyenes are known to undergo formylation with subsequent cyclisation. Both the carboxylic acid functionality and the butadiene moiety are present in 2,4-hexadienoic acids and they are easily prepared. The

easy accessibility of dienoic acids prompted us to explore the Vilsmeier reaction on these substrates. As expected, the dienoic acids under Vilsmeier reaction conditions gave substituted polyformylbenzenes through annelation of the resulting iminium salt intermediates.

A large number of ketones were subjected to Vilsmeier reaction[1] to give 3-chloroacroleins. Polyformylation of suitably substituted carbonyl compounds was achieved by using a large excess of the Vilsmeier reagent at elevated temperatures. The easy accessibility of substituted cyclohexenones prompted us to explore the Vilsmeier reaction on these substrates and indeed the present investigation afforded a facile method for the preparation of a rich structural variety of polyformylbenzenes.

As a direct route for the preparation of polyformylbenzenes, the above methodologies seem to be extremely facile.

The retrosynthetic analysis of sesquiterpenes, like pterosin M, onitin and onitisin as well as the complex plant product, quassin appears to lend to a common starting material, *viz.*, 2,6-dimethyl-3-hydroxyphenylacetic acid. Biogenetic reasoning suggests the monoterpenic origin of 2,6-dimethyl-3-hydroxyphenylacetic acid and 2,6-dimethyl-3,4-dihydroxyphenylacetic acid. The synthesis of these two acids was achieved, starting from 2,4-dimethylphenol and using *t*-butyl group as a positional protecting group. 2,6-Dimethyl-3-hydroxyphenylacetic acid was successfully elaborated to pterosin M and onitin by a series of reactions.

References

1. JUTZ, C. — In *Iminium salts in organic chemistry*, Part 1, 1976, pp. 225–342, Ed. Bohme and H. G. Viehe, John Wiley and Sons, New York.
2. BIRCH, A. J. AND SUBBA RAO, G. S. R. — In *Advances in organic chemistry*, 1972, Vol. 8, pp. 1–65, Ed. E. C. Taylor, John Wiley, New York.
3. RAJU, B. AND KRISHNA RAO, G. S. — Vilsmeier reaction of some 1-methoxy-1,4-cyclohexadienes: A convenient route to polyformylbenzenes, *Synthesis*, 1985, 779–81.
4. RAJU, B. AND KRISHNA RAO, G. S. — Conversion of 1,4-dihydrobenzoic acids to polyformylbenzenes under Vilsmeier reaction conditions, *Synthesis* (in press).

Thesis Abstract (Ph.D.)

Triacylglycerol synthesis in developing seeds of groundnut (*Arachis hypogaea*) by V. Sukumar.

Research supervisor: P. S. Sastry.
Department: Biochemistry.

1. Introduction

Economically groundnut is one of the most important crops of this country. Today India is the largest producer of groundnut and accounts for more than 30% of the world production. Considerable efforts have been made by plant breeders to increase the yield of this crop though with limited success. Therefore, yield increases by biochemical and genetic manipulations assume significance. In oil seeds, prerequisite to such an approach is an understanding of the

seed lipid metabolism - the enzyme pathways, the rate limiting steps, the levels of the enzymes during seed development and their regulation.

The photosynthate in plants is transported to the seeds exclusively in the form of sucrose[1,2]. It is in the seeds that this precursor is channelised to the storage product. In oil seeds, energy is stored mainly in the form of triacylglycerol. The mechanism of which such a selective channeling occurs in the developing seed is not known. It has been observed in various oil seeds that active accumulation occurs at a specific period in the development of the seed but the characteristics of the enzymes involved and their regulation have not been established. This investigation has been carried out to elucidate the pathway of triacylglycerol biosynthesis in the developing seeds of groundnut, characterise the enzymes involved and to study the changes in the levels of these enzymes during seed development.

2. Experimental programme

Groundnut seeds, obtained from the local market, were soaked in water for a few hours and then allowed to germinate on wet cotton for 2–3 days. The seedlings were then planted in pots and grown under field conditions. The plants flowered in 6–7 weeks after planting. Being a self-pollinating flower, the day of flowering was taken as the day of fertilization. Each plant was allowed to flower for 3 days. Flowers appearing before or after this period were removed. The age of the seeds was expressed in terms of days afer fertilization (DAF). Plants were uprooted at specified days after fertilization and the pods removed. These were then washed in tap water and the seeds were dissected out for the experiments.

The characteristics of the various enzymes involved in triacylglycerol synthesis were then determined using 30 DAF seeds. Fatty acid; CoA ligase was studied by monitoring the conversion of [1-^{14}C] palmitic acid to [1-^{14}C] palmitoyl CoA. The assay for *sn*-glycerol-3-phosphate acyltransferase involved monitoring the conversion of [^{32}P] DL-glycerol-3-phosphate to phosphatidic acid. The release of [^{32}Pi] orthophosphate from [^{32}P]-phosphatidic acid was taken as an index of phosphatidic acid phosphohydrolase activity. The diacylglycerol acyltransferase assay employed involved studying the acylation of *sn* 1,2-diacylglycerol by [9,10-^{3}H] Oleoyl CoA. The changes in the levels of these enzymes with age were also monitored.

3. Results and conclusions

The results presented in this thesis show that the site of triacylglycerol biosynthesis in the developing seed is pre-microsomes. All the enzymes converting *sn* glycerol-3-phosphate to triacylglycerol were shown to be maximally present in this organelle (Table I). The fat fraction did not contain significant enzymic activity. It has been suggested that the floating fat layer, obtained on homogenisation and subsequent centrifugation of the seed, contains oleosomes which are the sites of triacylglycerol synthesis[3]. To further confirm our findings which suggested that the oleosomes have only a storage function in the developing groundnut, studies on the chemical composition and protein pattern of these organelles were carried out. SDS-PAGE of the oleosomal proteins showed the presence of only 5 proteins ranging in molecular weight from 20,000 to 46,000 daltons. Secondly, the oleosomes were shown to contain only 0.65% of their dry weight as protein and only about 0.8% as phospholipids. It is, therefore, concluded that the oleosomes cannot have significant biosynthetic capacity with its limited repertoire of proteins. Fatty acid: CoA ligase, *sn*-glycerol-3-phosphate acyltransferase and phosphatidic acid phosphohydrolase were also present in significant amounts in the mitochondria. Whether the diacylglycerol formed in the mitochondria is translocated to the microsomes remains to be investigated. The

intracellular localisation of the various precursors and enzymes for triacylglycerol synthesis, based on our findings and that of an earlier study in this laboratory (4) is shown in fig. 1.

Table I
Subcellular localisation of the enzymes involved in triacylglycerol synthesis

Fraction	Enzyme activity, n moles/h/mg protein			
	Acyl-CoA synthetase	Glycerol 3 phosphate acyltransferase	Phosphatidic acid phosphatase	Diacylglycerol acyltransferase
Homogenate	192 ±14.1	9.69 ± 0.35	164 ±5.1	78.8±4.1
Nucleus	48.9±2.7	0.83 ± 0.13	30.3±0.8	25.6±2.2
Post-nuclear supernatant	358 ±3.4	17.57 ± 0.6	251 ±36	152 ±8.6
Mitochondria	999 ±77.8	838 ±4.1	1415 ± 116	135 ±12
Microsomes	2183 ±81.8	389.6 ± 33	1629 ± 21.5	1814 ±31
Cytosol	106 ±4.13	—	—	28.5 ±0 5
Fat layer	153 ±6.9	279 ±43	177 ±44	201 ±24

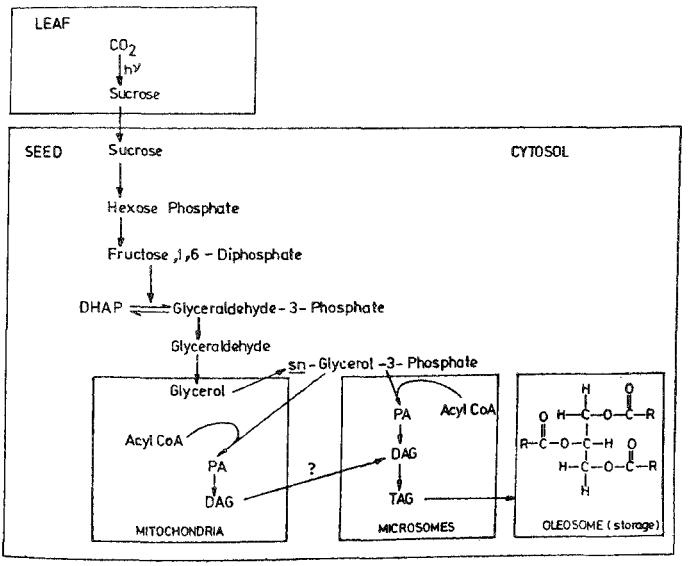

Fig 1. Intracellular localisation of the enzymes of triacylglycerol synthesis in developing groundnut seed.

Table II
Biosynthetic activities of triacylglycerol biosynthetic enzymes from microsomes of developing groundnut seed at 30–35 DAF

Sl No.	Enzyme	Activity μ moles/seed/day
1.	Fatty acid: CoA ligase	47
2.	*sn*-glycerol-3-phosphate acyltransferase	8.4
3.	Phosphatidic acid phosphohydrolase	35.1
4.	Diacylglycerol acyltransferase	39.6

The average protein/seed at the peak period of lipid accumulation (30–35 DAF) was 19 mg. Of this 0.91 mg was present in the microsomes. The activities of the enzymes were calculated as: Peak specific activity (n moles/h/mg protein × 0.91 × 24/1,000

During the peak period of lipid accumulation, *i.e.* 30–35 DAF, the developing groundnut seed makes 7–8 μ moles of oil/seed/day. It has been observed that glycerokinase is the rate-limiting step in the conversion of hexoses to *sn*-glycerol-3-phosphate and its activity during the 30–35 DAF period was estimated to be 42–45 μ moles/seed/day[4]. The biosynthetic activities of the other enzymes in the pathway, based on this study are given in Table II. It may be seen that *sn*-glycerol-3-phosphate acyltransferase is the rate-limiting step in the entire pathway from hexoses.

The development pattern of the various enzymes in the pathway, based on our study and that of a previous study in this lab, are shown in fig 2. It can be seen that all the enzymes involved

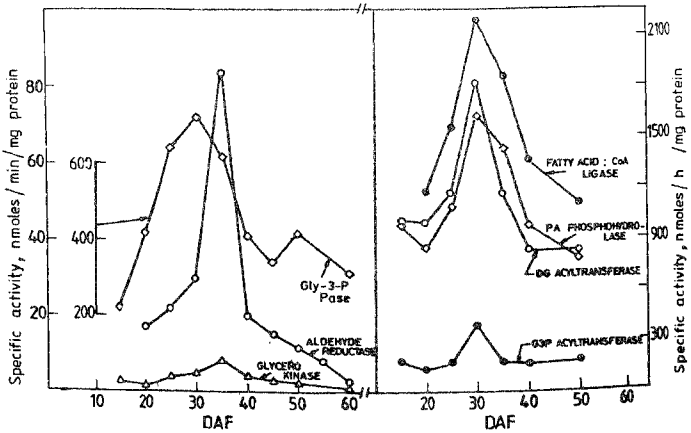

Fig 2. Developmental patterns of the enzymes of triacylglycerol biosynthesis.

show a peak of specific activity at 30–35 DAF when maximum lipid accumulation occurs suggesting the enzymes are coordinately regulated. This suggests that the regulation of oil synthesis in the developing groundnut is at the genetic level resulting in an increase in the synthesis of the enzyme activity by covalent modification as seen in many enzymes in the animal systems.

References

1. HATCH, M. D. AND GLASSIOER, K. T. — *Plant Physiol.*, 1964, **60**, 339.
2. GIAQUINTA, R. — *Plant Physiol.*, 1971, **60**, 339.
3. HARWOOD, J. L., SODJA, A., STUMPF, P. K. AND SPURR, A. R. — *Lipids*, 1971, **6**, 851.
4. GHOSH, S. — *Regulation of triacylglycerol synthesis in developing seeds of groundnut* (Arachis hypogaea): *Formation of* sn-*glycerol-3-phosphate*, Ph.D. thesis, Indian Institute of Science, Bangalore, India, 1985.